Applied Surface Science 256 (2010) 2143–2146

Contents lists available at ScienceDirect

Applied Surface Science

journal homepage: www.elsevier.com/locate/apsusc

Comparison of implantation and diffusion behavior of Ti, Sb and N in ion-implanted single crystal and polycrystalline ZnO: A SIMS study

J. Lee [a,*], J. Metson [b], P.J. Evans [c], U. Pal [d], D. Bhattacharyya [a]

[a] Department of Mechanical Engineering, The University of Auckland, 20 Symonds Street, Private Bag 92019, Auckland, New Zealand
[b] Department of Chemistry, The University of Auckland, Private Bag 92019, Auckland, New Zealand
[c] Australian Nuclear Science and Technology Organization, PMB 1, Menai, NSW 2234, Australia
[d] Instituto de Física, Universidad Autónoma de Puebla, Apdo. Postal J-48, Puebla, Pue. 72570, Mexico

ARTICLE INFO

Article history:
Received 27 May 2009
Received in revised form 29 July 2009
Accepted 18 September 2009
Available online 25 September 2009

Keywords:
Ion-implantation
SIMS
Dopant diffusion
ZnO

ABSTRACT

Implantation and diffusion behavior of Sb, Ti and N in ZnO single crystal and sputter deposited thin films were studied through secondary ion mass spectrometric studies on ion-implanted and thermally annealed samples. Sb was implanted and Ti and N were co-implanted into ZnO single crystals and polycrystalline thin films on Si substrates at room temperature. The implanted samples were then annealed at 800 °C. Depth profiles of implant distributions before and after annealing were examined by Secondary Ion Mass Spectrometry (SIMS). As expected, implant range is sensitive to the mass of the dopants; and the dopant distribution is broadened as implanted elements migrate deeper into the film on thermal annealing. While diffusion of N in the ZnO thin film is not significant, Ti tends to diffuse deeper into the sample during annealing. For Ti and N co-implanted single crystal, annealing induced diffusion causes more redistribution of the lighter N than Ti. In general, implanted dopants diffuse more easily in thin films compared to the single crystal due to the presence of grain boundaries in the latter.

1. Introduction

The wide band-gap material ZnO, normally an n-type semiconductor, has attracted much attention for optoelectronic applications in the visible and ultraviolet spectral regions such as in solar cells, gas sensing, as ultrasonic oscillators and transducers [1]. p–n junctions using p-type ZnO have possible applications in various electrical and optical devices like blue light emitting diodes, laser systems, etc. In this regard, a great effort has been devoted to prepare p-type ZnO by acceptor doping [2].

Ion-implantation is widely used for introducing conduction carriers into semiconductors, to realize selective-area doping, electrical and optical isolation, dry etching, and ion slicing [3]. Implantation of potential p-type dopants and co-implantation studies are beginning to show promising results for producing p-type ZnO [4]. Recently N as an acceptor and Al, Ga, and In as donors have been used as key dopants for preparing a p-/n-type semiconductors [5–7]. Park et al. [8] have reported the diffusion behavior of co-implanted nitrogen and indium into a ZnO single crystal after subsequent annealing at 800 °C in oxygen. Diffusion of N in the crystal was not detected, while In was observed to diffuse deeper into the crystal. Indium diffusion in implanted ZnO thin films was also demonstrated by Sakaguchi et al. [9]. Komatsu et al. found that for Ga and N co-implanted ZnO single crystals, annealing induces N and Ga diffusion deeper into the ZnO crystal, especially in the case of Ga [10]. There exist several mechanisms to explain the diffusion behavior of implanted elements in semiconductors, which are relevant to ZnO. Gerasimenko et al. have observed that the redistribution of implanted Mg and Be in InSb and InAs occurred between 350 and 450 °C, depending on the presence of other impurities [11]. In addition, Friesel et al. demonstrated that the diffusion of Sn in germanium follows the vacancy mechanism and depends on temperature [12].

TiN and Sb are potential p-type dopants in ZnO [13]. In this SIMS study, we focus on the implantation and diffusion behavior of TiN and Sb implanted in ZnO single crystals and thin film samples deposited by magnetron sputtering.

2. Experimental details

Low energy ion-implantation was carried out on ZnO thin films deposited on Si by r.f. magnetron sputtering and ZnO single crystals with a (0 0 0 1) surface (University wafer Inc.), using a metal vapor vacuum arc (MEVVA) ion source. TiN and Sb rods (>99.9% purity) were chosen as targets. The base pressure was 2×10^{-7} Pa. Ti + N and Sb were implanted at a dose of about 1×10^{16} ions/cm^2 at room temperature. An extraction voltage of 40 kV and ion beam current of 40 mA were used for the implantations.

* Corresponding author.
E-mail address: jl11018@gmail.com (J. Lee).

0169-4332/$ – see front matter © 2009 Elsevier B.V. All rights reserved.
doi:10.1016/j.apsusc.2009.09.064

After ion-implantation, the samples were subsequently annealed at 800 °C for 1 h in nitrogen atmosphere for Ti + N implanted samples, and under vacuum for Sb implanted samples. Depth profiling of each sample before and after annealing was carried out using a dynamic SIMS (CAMECA ims-5f) with $^{133}Cs^+$ as the primary ion, with a net accelerating voltage of 2.2 kV and a beam current of 15 nA. 55.0 μm diameter area of each of the samples was analyzed from the centre of a 250 μm × 250 μm area rastered by the primary ions. Secondary ions of interest were monitored as the MCs^+ adducts [13] with intensities normalized using the Cs^+ yield.

3. Results

The following results compare the behavior of different dopants in ZnO single crystal and thin film samples. Fig. 1 shows the depth profiles of N and Ti in co-implanted ZnO film before and after annealing. The results indicate that the lighter element N penetrated further compared to Ti. The boundary between the ZnO film and the Si substrate can be easily identified before annealing. Apparently, N and Ti concentrations peaked at around 20–30 nm depth. N penetration in the film may be assisted by the Zn rich defects [14] of n-type ZnO which favor the implantation of N ions. The N depth profile in the sample after annealing for 1 h in nitrogen revealed no change in dopant distribution. However, Ti shows high mobility in the ZnO thin film at high temperature as manifested by its redistribution after annealing at 800 °C (Fig. 1). After annealing, there occurred also an inter-diffusion at the boundary between the film and substrate. Some substrate derived Si appeared at the surface of the ZnO thin film. Diffusion of Ti deep into the ZnO film and extending to the film/substrate interface might be due to grain boundary diffusion.

The diffusion behavior of N and Ti in co-implanted ZnO single crystal before and after thermal annealing at 800 °C is shown in Fig. 2. Both Ti and N migrated into the sample after annealing to some extent; however, Ti seems to be less mobile than N. The observations are very different from that in the ZnO thin film.

The Sb and Si distributions in Sb implanted ZnO thin film, before and after thermal annealing are shown in Fig. 3. As expected, annealing induced the diffusion of the Sb into the film and led to a very broad Sb plateau region to a depth of 220 nm. In contrast, the mobility of Sb was low in ZnO single crystal (Fig. 4), where the distribution of Sb concentration did not change beyond 70 nm depth after thermal annealing. However, it might be possible that during annealing at 800 °C, Sb evaporated from the sample due to its high vapor pressure (100 Pa at 738 °C [15]) encouraged by its poor diffusion into the ZnO single crystal.

From our SIMS results, it is clear that thermal annealing caused less diffusion of dopants into the ZnO single crystal than in the polycrystalline thin films. This can be attributed to the absence of grain boundaries and fewer defects in the ZnO single crystal compared to the thin films. Increase of Si concentration at the film surface after thermal annealing in our ZnO films deposited on Si (Figs. 1–3) also suggests the role of grain boundary on dopant diffusion.

Cross-sectional SEM images of un-implanted and Ti + N co-implanted ZnO thin film before and after thermal annealing are presented in Fig. 5. Before implantation, the ZnO thin film deposited by magnetron sputtering on Si shows fine columnar nanocrystalline structures. Despite the use of low implantation energy, after implantation, the columnar crystalline structures appeared to be disrupted forming amorphous regions (Fig. 5b). However, after annealing at 800 °C, the structures recrystallized to form a coarse columnar morphology with damage remaining near the surface. Fig. 6 shows that XRD spectra of un-implanted and Ti + N co-implanted ZnO thin films before and after thermal

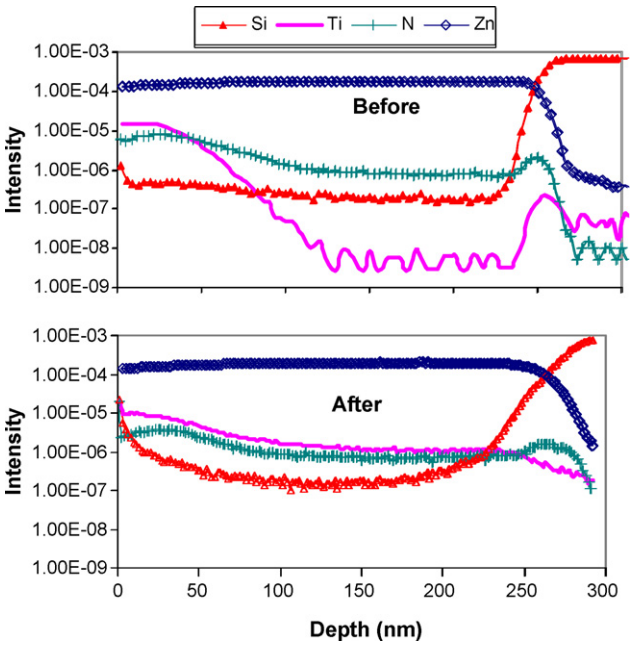

Fig. 1. Concentration depth profiles of N and Ti in the co-implanted ZnO thin films before and after annealing for 1 h at 800 °C.

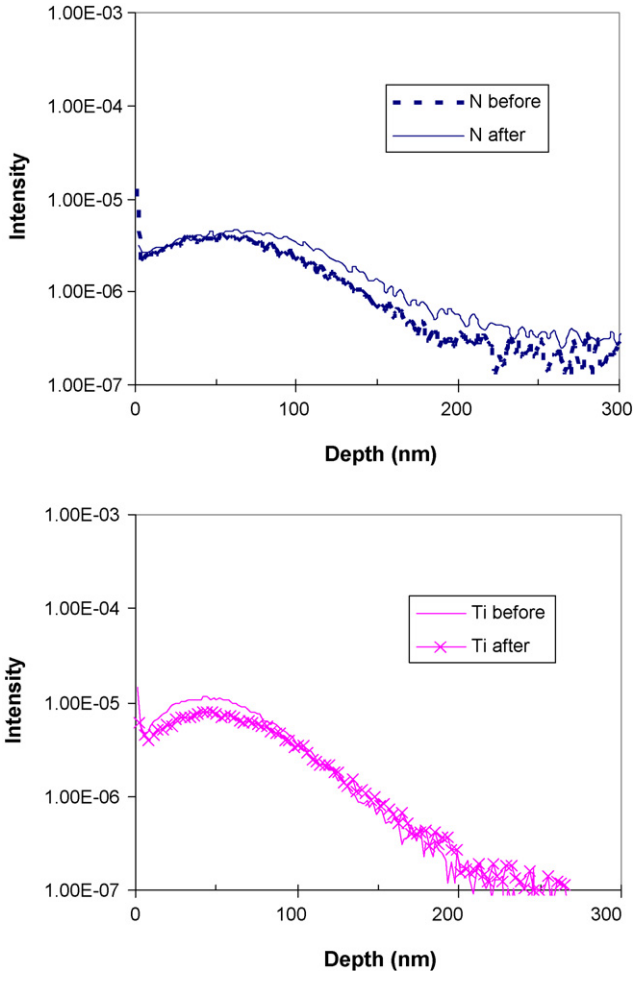

Fig. 2. Concentration depth profiles of N and Ti in the co-implanted ZnO single crystal before and after annealing for 1 h at 800 °C.

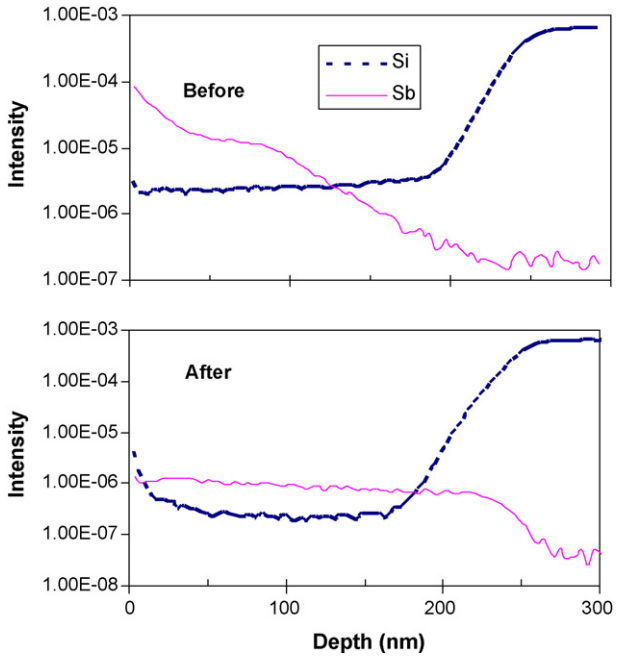

Fig. 3. Concentration depth profiles of Sb implanted ZnO thin films before and after annealing for 1 h at 800 °C.

annealing. After implantation, the *c*-axis orientation of the polycrystalline structure has been significantly decreased. However, after the thermal annealing, the *c*-axis orientation has been enhanced compared to the un-implanted ZnO thin film. This is attributed to the minimization of the surface energy favoring the texture along the *c*-axis [16,17].

4. Discussion

The concentration depth profile of implanted titanium and nitrogen has been shown in Fig. 1. The diffusion of N in the sample co-implanted with Ti and N, was not so significant after annealing of the ZnO thin film. The ionic radius of nitrogen (III) (132 pm) is the largest among those of Zn (II) (80 pm), Ti (III) (81 pm), and O (II) (120 pm) [18] which might be one of the reasons for poor diffusion of nitrogen into the ZnO thin films. The N-implanted ZnO could also form zinc oxynitride compounds [19], which can hinder the diffusion of N in the Ti + N co-implanted films under these experimental conditions. Nitride compounds are readily observed in N implanted metals [8]. Komatsu et al. [10] have demonstrated the enhancement of the N solubility limit by its coexistence with Ga in ZnO single crystals. In the Ti + N co-implanted ZnO single crystal, N shows some mobility. This is somewhat different from the observations of Park et al. [8] for their In + N co-implanted ZnO. It was proposed that the N occupied an O site in the N-doped ZnO thin film, but an interstitial site in the ZnO single crystal in the presence of Ti. Furthermore, the implanted Ti showed significantly more mobility in the ZnO thin film during annealing than in the ZnO single crystal. As Ti diffusion progressed during annealing, Ti distribution followed that of nitrogen in the ZnO thin film.

The implanted Sb profiles in the ZnO single crystal do not have a Gaussian shape under these implantation conditions. After annealing at 800 °C for 1 h, there is some evidence of Sb loss

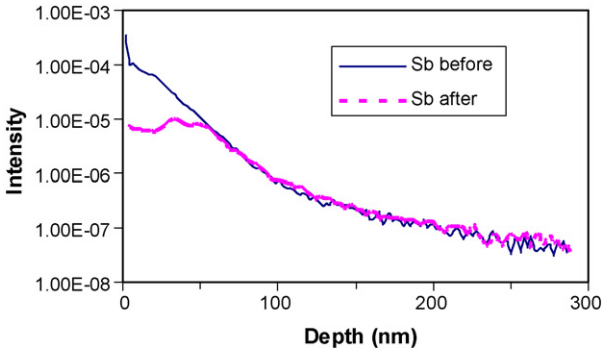

Fig. 4. The depth profiles of Sb implanted ZnO single crystal before and after annealing for 1 h at 800 °C.

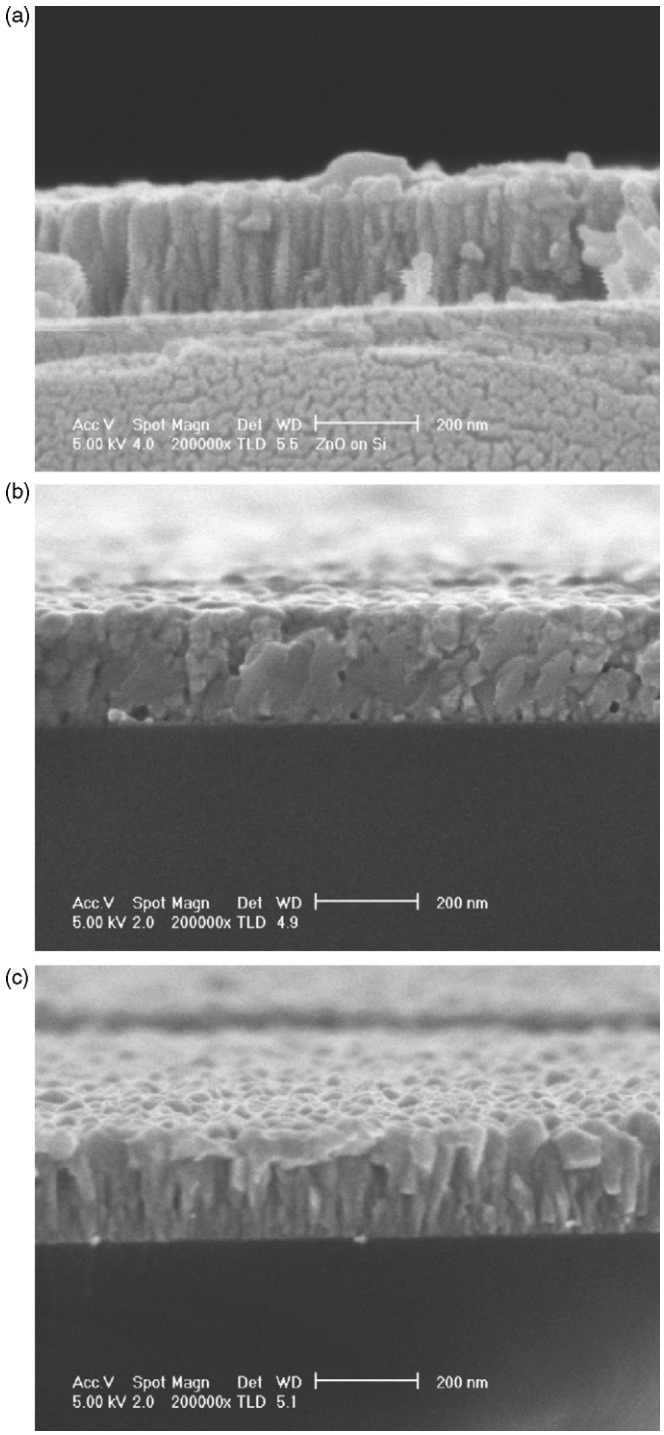

Fig. 5. SEM cross-section micrographs of un-implanted (a), TiN implanted before (b) and after annealing (c) of ZnO thin films.

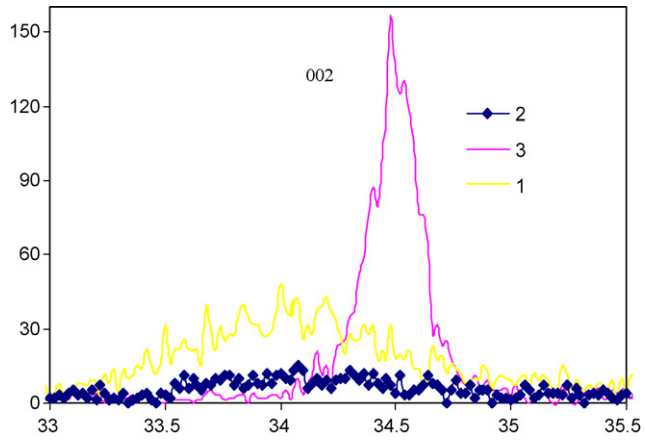

Fig. 6. XRD spectra (0 0 2 orientation) of un-implanted (1), TiN implanted before (2) and after annealing (3) of ZnO thin films deposited on Si.

through gas phase and a small peak in the concentration depth profile of Sb is formed at a depth of around 30–50 nm. It is considered that these layers are related to Sb diffusion and the swelling surface layer (defective surface area) [11] under annealing at 800 °C in the ZnO single crystal. However in the ZnO thin film, recrystallization and residual defects generated by implantation make Sb to diffuse more easily, resulting in a very broad plateau in the depth profiles (Fig. 3). The Ti and N also have a broad plateau in the depth profile for the Ti + N co-implanted ZnO thin film. Not surprisingly, dopants diffuse more easily in the ZnO thin film compared to a single crystal. This is similar to the observation of Mg diffusion in InSb [11].

From the shape of the depth profiles, we can observe that the diffusion plateau of Sb in the ZnO single crystal is somewhat similar to that of In implanted in a ZnO single crystal [9]. Accelerated migration of dopants along the *c*-axis observed in our ZnO thin films might be attributed to their columnar crystalline structure.

SEM and XRD results indicated that the implantation induced distortion of the columnar structures of the ZnO thin films. However, after thermal annealing, the structures recrystallize to form a coarse columnar morphology.

5. Summary

The implantation and diffusion behavior of Sb, Ti and N in ZnO thin film and single crystal samples during annealing at 800 °C was investigated by ion-implantation at low energy (40 kV). In as implanted thin film samples, the implant concentrations exhibit maxima at around 20–50 nm depth. While the diffusion of N in ZnO thin film was not significant, Ti diffuses deeper into the sample during annealing. For Ti and N co-implanted ZnO single crystal, the implanted species concentrated at around 60 nm depth in the sample. However, annealing induced diffusion caused more redistribution of the lighter N than heavier Ti. The diffusion behavior of Sb is quite different in ZnO single crystal from ZnO thin films. Implanted dopants diffused more easily in thin film than in single crystal. Implantation disrupted the columnar crystalline structure of ZnO thin films, which can be recovered on thermal annealing. The *c*-axis oriented columnar structures of ZnO thin film helped the migration of the implanted dopants along the *c*-axis. Further study on the annealing at several temperatures is needed to understand their diffusion behavior in detail.

Acknowledgements

J. Lee would like to thank New Zealand Tertiary Education Commission (Bright Future Doctoral Scholarship), Doctoral Scholarship of The University of Auckland and the Australian Institute of Nuclear Science and Engineering (Postgraduate Award). We acknowledge the assistance of R.A. Russell, D. Button, SIMS Group (ANSTO, Australia) and Research Centre for Surface and Material Science, The University of Auckland.

References

[1] T. Aoki, Y. Hatanaka, D.C. Look, Applied Physics Letters 76 (2000) 3257–3258.
[2] D.C. Look, D.C. Reynolds, C.W. Litton, R.L. Jones, D.B. Eason, G. Cantwell, Applied Physics Letters 81 (2002) 1830–1832.
[3] S.O. Kucheyev, J.S. Williams, C. Jagadish, Vacuum 73 (2004) 93–104.
[4] T. Yamamoto, Thin Solid Films 420–421 (2002) 100–106.
[5] J.G. Lu, Z.Z. Ye, F. Zhuge, Y.J. Zeng, B.H. Zhao, L.P. Zhu, Applied Physics Letters 85 (2004) 3134–3135.
[6] J.M. Bian, X.M. Li, X.D. Gao, W.D. Yu, L.D. Chen, Applied Physics Letters 84 (2004) 541–543.
[7] M. Joseph, H. Tabata, H. Saeki, K. Ueda, T. Kawai, Physica B: Condensed Matter 302–303 (2001) 140–148.
[8] D.-C. Park, I. Sakaguchi, N. Ohashi, S. Hishita, H. Haneda, Applied Surface Science 203–204 (2003) 359–362.
[9] I. Sakaguchi, D. Park, Y. Takata, S. Hishita, N. Ohashi, H. Haneda, T. Mitsuhashi, Nuclear Instruments and Methods in Physics Research Section B: Beam Interactions with Materials and Atoms 206 (2003) 153–156.
[10] M. Komatsu, N. Ohashi, I. Sakaguchi, S. Hishita, H. Haneda, Applied Surface Science 189 (2002) 349–352.
[11] N.N. Gerasimenko, G.S. Khryashchev, G.L. Kuryshev, A.M. Myasnikov, V.I. Obodnikov, Nuclear Instruments and Methods in Physics Research Section B: Beam Interactions with Materials and Atoms 111 (1996) 281–284.
[12] M. Friesel, U. Sodervall, W. Gust, Journal of Applied Physics 78 (1995) 5351–5355.
[13] G. Xiong, K.B. Ucer, R.T. Williams, J. Lee, D. Bhattacharyya, J. Metson, P. Evans, Journal of Applied Physics 97 (2005) 043528–43534.
[14] S. Dogan, A. Ates, G. Xiong, J. Wilkinson, S. Tuzemen, M. Yildirim, R.T. Williams, Physica Status Solidi A: Applied Research 195 (2003) 165–170.
[15] D.R. Lide, Handbook of Chemistry and Physics, vol. 79th, CRC, 1998–1999.
[16] Y.X. Liu, Y.C. Liu, D.Z. Shen, G.Z. Zhong, X.W. Fan, X.G. Kong, R. Mu, D.O. Henderson, Journal of Crystal Growth 240 (2002) 152–156.
[17] J.F. Chang, W.C. Lin, M.H. Hon, Applied Surface Science 183 (2001) 18–25.
[18] http://www.webelements.com.
[19] M. Futsuhara, K. Yoshioka, O. Takai, Thin Solid Films 317 (1998) 322–325.